INTERNAL BALLISTICS CALCULATIONS OF THE SOLID PROPELLANT ROCKET ENGINE WITH TWO COMBUSTION CHAMBERS

The Dung Nguyen[1,*], Ngoc Thanh Dang[1], Ngoc Du Nguyen[2]

[1]*Le Quy Don Technical University, Hanoi, Vietnam*
[2]*Military Institute of Science and Technology, Hanoi, Vietnam*

Abstract

The paper presents the theoretical modeling of the internal ballistics properties of the solid propellant rocket engine with two combustion chambers. From the working characteristics of the solid propellant rocket engine with two combustion chambers and the theory of a solid propellant rocket engine, a system of equations that describes the processes that occur in the combustion chambers of the engine is established. Provide a method to solve the system of equations and necessary boundary conditions. Solve problems on model engines and verify theoretical results by experimental studies. The error between experimental studies and theoretical calculation is relatively small (less than 10%), confirming the reliability of the built mathematical model. Research results serve the design calculation and manufacture of the solid propellant rocket engine with two combustion chambers.

Keywords: *Solid rocket engine; interior ballistics calculations; two combustion chambers.*

1. Introduction

The solid rocket engine with two combustion chambers is a type of solid rocket engine with two combustion chambers, two propellant grains, two igniters, one common nozzle, and a separation device. The separation device protects the second combustion chamber from being ignited while the propellant grain of the first combustion chamber burns. Upon ignition of the second combustion chamber, the separation device opens and allows the gas to exhaust through the first combustion chamber and the nozzle. The principle schematic of the solid rocket engine with two combustion chambers is shown in Fig. 1.

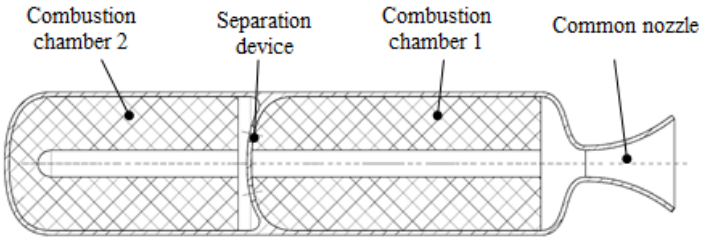

Fig. 1. Principle schematic of the solid rocket engine with two combustion chambers

* Email: nguyentd.mta@gmail.com

Depending on time ignition propellant grain in the second combustion chamber, the rocket engine may have the following working modes:

Case 1: The propellant grain in the second combustion chamber is ignited after a slow hold Δt from the moment combustion chamber 1 ends its operation. The working result of the engine in this case produces two different thrust pulses with the interval of Δt (Fig. 2). This is the typical case in practice

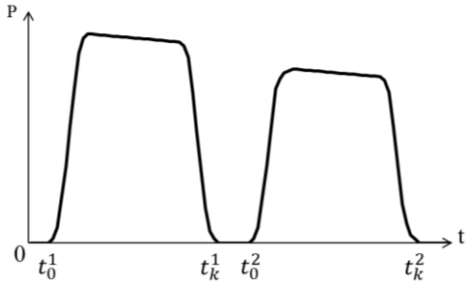

Fig. 2. Two pulses thrust mode of the solid rocket engine with two combustion chambers

Case 2: The propellant grain in the second combustion chamber is ignited while the first combustion chamber is active. The engine's working results generate a thrust pulse (single pulse) with different possible thrusting modes corresponding to the combustion phases of the two propellant grains in the two combustion chambers (Fig. 3).

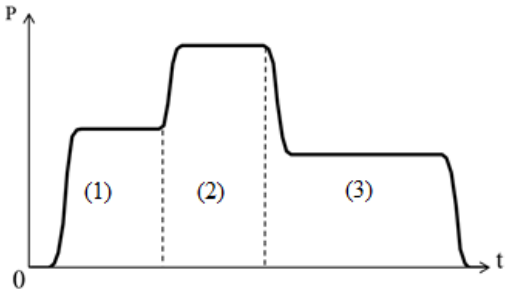

Fig. 3. One pulse thrust mode of the solid rocket engine with two combustion chambers

1- Individual burning phase of propellant grain in combustion chamber 1

2- The burning phase of both propellant grains in two combustion chamber

3- Individual burning phase of propellant grain in combustion chamber 2

With these characteristics, it attracts attention when studying structural solutions for guided missiles in the limited conditions of propellant grains manufacturing technology.

The purpose of this research is to establish an initial theoretical basis for the study of a solid rocket engine with two combustion chambers. In the paper, the theoretical research method is used in combination with the experimental research.

2. Mathematical model

2.1. Basic assumptions

The working process of the engine is investigated under the following conditions with the following basic assumptions:

1) The transition period into the engine working mode that occurs in the closed volume of the combustion chambers for a very short time, does not significantly affect the working characteristics of the engine. Therefore, it is assumed that the free surfaces of each propellant grain are ignited simultaneously and instantaneously at the time that the powder is burned off and the diaphragm of the nozzle is opened (with the combustion chamber 1) or that the powder is burned off and the window on separation device is opened (with the combustion chamber 2).

2) The combustion product area is disturbed by the flow of the hot gas through the window on the separation device, which accounts for a small quantity, which can be ignored compared with the free volume of the combustion chambers.

3) The stuffing conditions in the two combustion chambers are guaranteed to appear with a small intensity of the erosive burning effect, the combustion products in the combustion chambers are almost stationary, and the parameters of states averaged over the free volume of each combustion chamber.

4) The propellant grains are ballistite and can consider the thermodynamic characteristics specific heat capacity isotonic c_v, specific heat capacity isotope $c_{p,}$ and gas constant R of the hot gas in both combustion chambers are the same.

5) The combustion product in the combustion chambers does not contain solid or liquid particles, has completely completed the combustion reactions, can be considered as an ideal gas.

6) The thermodynamic processes occurring in the combustion chambers and the nozzle are isentropic and one-dimensional flow.

2.2. Equations describing the processes occurring in the engine

Applying the schematic with the above conceptions and assumptions, it is possible to set up equations describing the processes occurring inside the combustion chambers, as a basis for simulation to examine the operating modes of the solid rocket engine with two combustion chambers.

The combustion process and movement of combustion product in the combustion chambers comply with the following equations:

- Equation of burning and gas generation of propellant grains;

- The mass conservation equation;

- The energy conservation equation;
- Equations of state.

2.2.1. Equation of burning and gas generation of propellant grains

The combustion of propellant grains is a major factor in engine performance and is characterized by the burning rate at which the combustion product masses the heat into the combustion chambers [1, 5, 6]:

Combustion chamber 1

$$\dot{m}_1^+ = \frac{dm_1^+}{dt} = \rho_{T1} S_1(e)\, u_{11}\, p_1^{\nu_1} \quad (1)$$

$$S_1 = S_1(e) \quad (2)$$

$$u_{LP1} = \left(\frac{de}{dt}\right)_{LP1} = u_{11} p_1^{\nu_1} \quad (3)$$

Combustion chamber 2

$$\dot{m}_2^+ = \frac{dm_2^+}{dt} = \rho_{T2} S_2(e)\, u_{12}\, p_2^{\nu_2} \quad (4)$$

$$S_2 = S_2(e) \quad (5)$$

$$u_{LP2} = \left(\frac{de}{dt}\right)_{LP2} = u_{12} p_2^{\nu_2} \quad (6)$$

where $\dot{m}_1^+, \dot{m}_2^+$ are gas flow rates generated of propellant grains in the combustion chamber 1 and 2; S_1, S_2 are the burning surface areas of propellant grains in the combustion chamber 1 and 2; u_{LP1}, u_{LP2} are the burning rates of propellant grains in the combustion chamber 1 and 2; u_{11}, u_{12} are coefficients of burning rate in the law of the burning rate of the propellant grains in the combustion chamber 1 and 2; ν_1, ν_2 are burning rate exponents of the propellant grains in the combustion chamber 1 and 2; ρ_{T1}, ρ_{T2} are densities of the propellant grains in the combustion chamber 1 and 2; p_1, p_2 are pressures in the combustion chamber 1 and 2.

2.2.2. The mass conservation equation

At the moment *t*, the mass of the product in the combustion chamber 1 is m_1 and in chamber 2 is m_2. According to the law of conservation of mass, we have:

$$\dot{m}_1 = \dot{m}_1^+ - \dot{m}_1^- + \delta_3 \dot{m}_{tr.d} \quad (7)$$

$$\dot{m}_2 = \dot{m}_2^+ - \delta_3 \dot{m}_{tr.d} \quad (8)$$

where $\dot{m}_1, \dot{m}_2$ are mass flow rates of combustion product in the combustion chamber 1 and 2; $\dot{m}_1^-$ is mass flow rate of the combustion product exiting the nozzle; $\dot{m}_{tr.d}$ is mass flow rate of combustion products exchanged between the two combustion chambers through the window in the separation device.

The mass flow rate of the combustion product exiting the nozzle is determined by a common formula in rocket engine theory [1, 4].

$$\dot{m}_1^- = \frac{dm_1^-}{dt} = \frac{\varphi_2 K_0(k) F_{th} p_1}{\sqrt{RT_{g.1}}} \tag{9}$$

where φ_2 is the loss coefficient of the combustion product flow through the nozzle; F_{th} is throat area of the nozzle; R is gas constant of the combustion product; k is the adiabatic exponent of the combustion product; $K_0(k)$ is function of adiabatic exponent.

$$K_0(k) = \left(\frac{2}{k+1}\right)^{\frac{1}{k-1}} \sqrt{\frac{2k}{k+1}}$$

The mass flow rate of exchanging the mass of the combustion product between two combustion chambers through the window on the separation device is determined by the cross-sectional area F_{lt} of the window on the separation device and the relationship between the pressures p_1 and p_2 in the combustion chamber 1 and combustion chamber 2. According to the [1, 3], we have:

$$\dot{m}_{tr.d} = \begin{cases} \dfrac{\varphi_2 F_{lt} p_2}{\sqrt{RT_{g.2}}} \sqrt{\dfrac{2k}{k-1}\left[\left(\dfrac{p_1}{p_2}\right)^{\frac{2}{k}} - \left(\dfrac{p_1}{p_2}\right)^{\frac{k+1}{k}}\right]} & \text{, when } 1 < \dfrac{p_2}{p_1} < \left(\dfrac{k+1}{2}\right)^{\frac{k}{k-1}} \\ \dfrac{\varphi_2 K_0(k) F_{lt} p_2}{\sqrt{RT_{g.2}}} & \text{, when } \dfrac{p_2}{p_1} \geq \left(\dfrac{k+1}{2}\right)^{\frac{k}{k-1}} \\ \dfrac{\varphi_2 F_{lt} p_1}{\sqrt{RT_{g.1}}} \sqrt{\dfrac{2k}{k-1}\left[\left(\dfrac{p_2}{p_1}\right)^{\frac{2}{k}} - \left(\dfrac{p_2}{p_1}\right)^{\frac{k+1}{k}}\right]} & \text{, when } 1 < \dfrac{p_1}{p_2} < \left(\dfrac{k+1}{2}\right)^{\frac{k}{k-1}} \\ \dfrac{\varphi_2 K_0(\mathrm{k}) F_{lt} p_1}{\sqrt{RT_{g.1}}} & \text{, when } \dfrac{p_1}{p_2} \geq \left(\dfrac{k+1}{2}\right)^{\frac{k}{k-1}} \end{cases} \tag{10}$$

where $T_{g.1}, T_{g.2}$ are temperature of combustion product in the combustion chamber 1 and 2; F_{lt} is cross-sectional area of the window on the separation device; φ_2 is the loss coefficient of mass flow; δ_3 is coefficient determines the direction of the flow through the separation device.

$$\delta_3 = \begin{bmatrix} 1, & \text{when } p_2 > p_1 \\ -1, & \text{when } p_2 < p_1 \\ 0, & \text{when } p_2 = p_1 \end{bmatrix}$$

2.2.3. The energy conservation equation

Give $dI_{tr.d}$ is the enthalpy variation of the exchanged gas between combustion

chamber 2 and combustion chamber 1, then we have [1]:

$$dI_{tr.d} = \begin{cases} \dot{m}_{tr.d} c_p \, \mathrm{T}_{g.2} \mathrm{dt}, \text{ when } p_2 > p_1 \\ \dot{m}_{tr.d} c_p \, \mathrm{T}_{g.1} \mathrm{dt}, \text{ when } p_2 < p_1 \\ 0, \text{ when } p_2 = p_1 \end{cases} \quad (11)$$

where c_p is specific heat capacity isotope in the combustion chamber 1 and combustion chamber 2.

The energy conservation equation for combustion chamber 1 and combustion chamber 2 is built based on the law of thermodynamic I:

a. For combustion chamber 1

$$dQ_1 + \delta_3 dI_{tr.d} = dU_1 + \sum dl_1 \quad (12)$$

where Q_1 is total energy of gas generated in combustion chamber 1, is determined by the expression:

$$dQ_1 = \left(dm_1^+\right) c_v T_{1.1} = \dot{m}_1^+ c_v T_{1.1} \quad (13)$$

where c_v is specific heat capacity isotonic in the combustion chambers; $T_{1.1}$ is the burning temperature of the propellant in the combustion chambers 1

U_1 is the energy of the gas in the combustion chamber 1, is determined by the expression:

$$dU_1 = d\left[\left(m_1^+ - m_1^- + \delta_3 m_{tr.d}\right) c_v T_{g.1}\right] \quad (14)$$

l_1 is the work of the gas flow in the combustion chamber 1, is determined by the expression:

$$\sum dl_1 = dm_1^- c_p T_{g.1} + dQ_{nh1} \quad (15)$$

Q_{nh1} is the heat of the hot gas transmitted to the combustion chamber 1 wall, is determined as follows:

$$dQ_{nh1} = \sum F_1 \alpha_1 (T_{g.1} - T_{K.1}) dt \quad (16)$$

where F_1 is surface area contacted to hot gas in the combustion chamber 1; $T_{K.1}$ is internal surface temperature of the combustion chamber wall 1; α_1 is coefficient of heat transfer from the combustion product to the combustion chamber wall 1.

Put (16), (15), (14), (13) into (12), we get:

$$\frac{dT_{g.1}}{dt} = \frac{1}{m_1^+ - m_1^- + \delta_3 m_{tr.d}} \left[\dot{m}_1^+ T_{1.1} - \dot{m}_1^- k T_{g.1} - \left(\dot{m}_1^+ - \dot{m}_1^- + \delta_3 \dot{m}_{tr.d}\right) T_{g.1} + \delta_3 \frac{(k-1)}{R} \frac{dI_{tr.d}}{dt} - \frac{(k-1)}{R} \frac{dQ_{nh1}}{dt}\right] \quad (17)$$

b. For combustion chamber 2

Applying the energy conservation equation for combustion chamber 2, we have:

$$dQ_2 - \delta_3 dI_{tr.d} = dU_2 + \sum dl_2 \quad (18)$$

Q_2 is total energy of gas generated in combustion chamber 2, is determined by the expression:

$$dQ_2 = \left(dm_2^+\right) c_v T_{1.2} = \dot{m}_2^+ c_v T_{1.2} dt \quad (19)$$

where $T_{1.2}$ is the burning temperature of the propellant in the combustion chambers 2; U_2 is the energy of the gas in the combustion chamber 2, is determined by the expression:

$$dU_2 = d\left[\left(m_2^+ - \delta_3 m_{tr.d}\right) c_v T_{g.2}\right] \quad (20)$$

l_2 is the work of the gas flow in the combustion chamber 2, is determined by the expression:

$$\sum dl_2 = dQ_{nh2} \quad (21)$$

Q_{nh2} is the heat of the hot gas transmitted to the combustion chamber 2 wall, is determined as follows:

$$dQ_{nh2} = \sum F_2 \alpha_2 (T_{g.2} - T_{K.2}) dt \quad (22)$$

where F_2 is surface area contacted to hot gas in the combustion chamber 2; $T_{K.2}$ is internal surface temperature of the combustion chamber wall 2; α_2 is coefficient of heat transfer from the combustion product to the combustion chamber wall 2;

Put (22), (21), (20), (19) in to (18), we get:

$$\frac{dT_{g.2}}{dt} = \frac{1}{m_2^+ - \delta_3 m_{tr.d}} \left[\dot{m}_2^+ T_{1.2} - \left(\dot{m}_2^+ - \delta_3 \dot{m}_{tr.d}\right) T_{g.2} - \delta_3 \frac{(k-1)}{R_1} \frac{dI_{tr.d}}{dt} - \frac{(k-1)}{R_1} \frac{dQ_{nh2}}{dt} \right] \quad (23)$$

2.2.4. Equations of state

Applying the equation of state of the gas to the combustion chambers, we get:

a. For combustion chamber 1

$$p_1 V_1 = m_1 R T_{g.1} \quad (24)$$

where V_1 is gas volume in combustion chamber 1.

Take the derivative over time equation (24), we get:

$$\dot{m}_1 = \frac{d}{dt}\left(\frac{p_1 V_1}{R T_{g.1}}\right) = \frac{V_1}{R T_{g.1}} \frac{dp_1}{dt} + \frac{p_1}{R T_{g.1}} \frac{dV_1}{dt} - \frac{p_1 V_1}{R T_{g.1}^2} \frac{dT_{g.1}}{dt}$$

With attention: $\frac{dV_1}{dt} = S_1 u_{Lp1}$ (25)

We have (26):

$$\frac{dp_1}{dt} = \frac{1}{V_1}\left[RT_{g.1}\left(\dot{m}_1^+ - \dot{m}_1^- + \dot{m}_{tr.d}\right) - p_1 S_1 u_{Lp1} + \frac{p_1 V_1}{T_{g.1}}\frac{dT_{g.1}}{dt}\right] \quad (26)$$

b. For combustion chamber 2

$$p_2 V_2 = m_2 R T_{g.2} \quad (27)$$

where V_2 is gas volume in combustion chamber 2.

In the same way to the combustion chamber 1, the differential equation is obtained as follows:

$$\frac{dp_2}{dt} = \frac{1}{V_2}\left[RT_{g.2}\left(\dot{m}_2^+ - \dot{m}_{tr.d}\right) - p_2 S_2 u_{Lp2} + \frac{p_2 V_2}{T_{g.2}}\frac{dT_{g.2}}{dt}\right] \quad (28)$$

2.3. System of equations of interior ballistic

From the above equations, we can get a system with 12 differential equations describing the interior ballistic of the solid rocket engine with two combustion chambers.

$$\begin{cases}
\frac{de_{c.1}}{dt} = \delta_1 u_{Lp1} = \delta_1 u_{11} p_1^{\nu_1} \\
\frac{dm_1^+}{dt} = \delta_1 S_1 u_{Lp1}\rho_{T1} = \delta_1 \rho_{T1} S_1(e)\,\mathrm{u}_{11}\, p_1^{\nu_1} \\
\frac{dp_1}{dt} = \frac{1}{V_1}\left[RT_{g.1}\left(\dot{m}_1^+ - \dot{m}_1^- + \delta_3\dot{m}_{tr.d}\right) - \delta_1 p_1 S_1 u_{Lp1} + \frac{p_1 V_1}{T_{g.1}}\frac{dT_{g.1}}{dt}\right] \\
\frac{dm_1^-}{dt} = \frac{\varphi_2 K_0(k) F_{th} p_1}{\sqrt{RT_{g.1}}} \\
\frac{dm_{tr.d}}{dt} = \dot{m}_{tr.d} \\
\frac{dT_{g.1}}{dt} = \frac{1}{m_1^+ - m_1^- + \delta_3 m_{tr.d}}\left[\dot{m}_1^+ T_{1.1} - \dot{m}_1^- k T_{g.1} - \left(\dot{m}_1^+ - \dot{m}_1^- + \delta_3\dot{m}_{tr.d}\right)T_{g.1} + \delta_3\frac{(k-1)}{R}\frac{dI_{tr.d}}{dt} - \frac{(k-1)}{R}\frac{dQ_{nh1}}{dt}\right] \\
\frac{dQ_{nh1}}{dt} = \sum F_{xq1}\alpha_1\left(T_{g.1} - T_{K.1}\right) \\
\frac{de_{c2}}{dt} = \delta_2 u_{Lp2} = \delta_2\,\mathrm{u}_{12}\, p_2^{\nu_2} \\
\frac{dm_2^+}{dt} = \delta_2 S_2 u_{Lp2}\rho_{T2} = \delta_2 \rho_{T2} S_2(e)\,\mathrm{u}_{12}\, p_2^{\nu_2} \\
\frac{dp_2}{dt} = \frac{1}{V_2}\left[RT_{g.2}\left(\dot{m}_2^+ - \delta_3\dot{m}_{tr.d}\right) - \delta_2 p_2 S_2 u_{Lp2} + \frac{p_2 V_2}{T_{g.2}}\frac{dT_{g.2}}{dt}\right] \\
\frac{dT_{g.2}}{dt} = \frac{1}{m_2^+ - \delta_3 m_{tr.d}}\left[\dot{m}_2^+ T_{1.2} - \left(\dot{m}_2^+ - \delta_3\dot{m}_{tr.d}\right)T_{g.2} - \delta_3\frac{(k-1)}{R}\frac{dI_{tr.d}}{dt} - \frac{(k-1)}{R}\frac{dQ_{nh2}}{dt}\right] \\
\frac{dQ_{nh2}}{dt} = \sum F_{xq2}\alpha_2\left(T_{g.2} - T_{K.2}\right)
\end{cases}$$

The coefficients δ_1, δ_2 are used to determine the ignition timing of the propellant grains:

$$\delta_1 = \begin{bmatrix} 1, \text{ when } 0 \le (e)_{LP1} < e_{11} \\ 0, \text{ when } (e)_{LP1} \ge e_{11} \end{bmatrix}; \qquad \delta_2 = \begin{bmatrix} 1, \text{ when } 0 \le (e)_{LP2} < e_{12} \\ 0, \text{ when } (e)_{LP2} \ge e_{12} \end{bmatrix}$$

2.4. Solution method

The system of equations can be solved to obtain the thermodynamic parameters of the combustion products using the 4th order Runge-Kutta method on the Matlab software platform. This is one of the popular methods, for reliable numerical solutions, to find the solutions of differential equations of the numerical analysis problems.

3. Results and experimental verification

3.1. Sample engines

Structure scheme of the sample engine used for calculation is shown on Fig. 4.

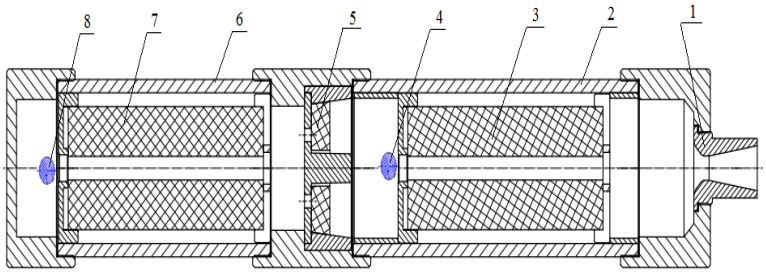

Fig. 4. Structure scheme of the sample engine

1 - Nozzle; 2 - Combustion chamber 1; 3 - Propellant grain 1; 4 - Igniter 1; 5 - Separation device; 6 - Combustion chamber 2; 7 - Propellant grain 2; 8 - Igniter 2.

In which, the separation device is made up of a metal part with the holes and the propellant grain has the same type as compared to the fuel dose propellant grain in combustion chambers.

The main structural parameters of the sample engine are presented in Table 1.

Table 1. Main structural parameters of the sample engine

Parameter	**Combustion chamber 1**	**Combustion chamber 2**
Length, [m]	0.292	0.292
Diameter, [m]	0.114	0.114
Length of propellant grain , [m]	0.2	0.2
Outside diameter of propellant grain, [m]	0.104	0.104
Inside diameter of propellant grain, [m]	0.018	0.018
Mark of the propellant grain	RSI-12M	RSI-12M
Diameter of throat section of the nozzle, [m]	0.018	

Structural parameters of the separation device are shown in Fig. 5.

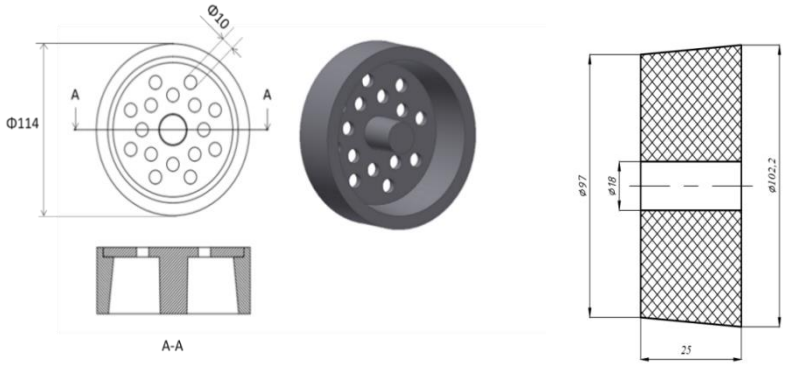

Fig. 5. Structural parameters of the separation device

The thermodynamic data of the propellant grain RSI-12M were extracted from [2] and determined using the ASTRA software. This is a software for calculating combustion in rocket engines, has been widely used in design and manufacture of missiles in the Russian Federation and is being used in Vietnam. Characteristic parameters are presented in Table 2.

Table 2. Characteristic parameters of propellant grain RSI-12M

No	Parameter	Symbol	Value	Unit
1	Burning temperature of the propellant grain	$T_{1.1}$, $T_{1.2}$	2731	K
2	Adiabatic exponent of the combustion product	k	1.25	
3	Gas constant of the combustion product	R	362	J/kg.K
4	Coefficient of burning rate	u_{11}, u_{12}	$43.44 \cdot 10^{-6}$	m/s
5	Burning rate exponent	ν_1, ν_2	0.3456	
6	Density of the propellant grains	ρ_{T1} , ρ_{T2}	1570	kg/m^3

The initial conditions:

The initial conditions when $t = 0$

$$\begin{cases} (e)_{LP1} = 7.23e-04\text{m} \\ m_1^+ = 0.082\,\text{kg} \\ p_1 = 4\,\text{MPa}\,,\ p_2 = p_0 \\ T_{g.1} = T_{1.1},\ T_{g.2} = T_0 \\ Q_{nh.1} = 0 \\ V_1 = V_{1.0} \end{cases}$$

The conditions when $t = t_{mlt}$

$$\begin{cases} (e)_{LP2} = 6.85e-04\text{m} \\ m_2^+ = 0.075\,\text{kg} \\ p_2 = 4\,\text{MPa} \\ T_{g.2} = T_{1.2} \\ Q_{nh.2} = 0; \\ V_2 = V_{2.0} \end{cases}$$

where p_{moi} is pressure of ignition in the combustion chambers; p_0, T_0 are the initial pressure and temperature in the combustion chamber, approximately equal to the

ambient pressure and temperature; $V_{1.0}$, $V_{2.0}$ are the initial free volumes of combustion chambers 1 and 2.

3.2. Result of calculation

Perform the solution of the system of equations with the sample engine in the case combustion chamber 2 is activated after the first combustion chamber has finished for a period of 1 s, similar to Fig. 2.

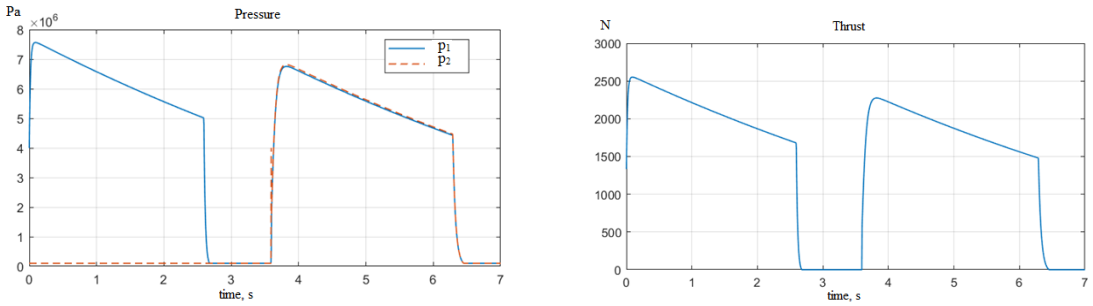

Fig. 6. Result of calculation

Combustion chamber 1 has a shorter working time than combustion chamber 2 and the average pressure is higher than combustion chamber 2, due to the simultaneous burning of the propellant grain in the separation device. So the average thrust of the engine in phase 2 is lower than the average thrust of the engine in phase 1.

3.3. Experimental results on the sample engine

Scheme of the test stand is shown in Fig. 7.

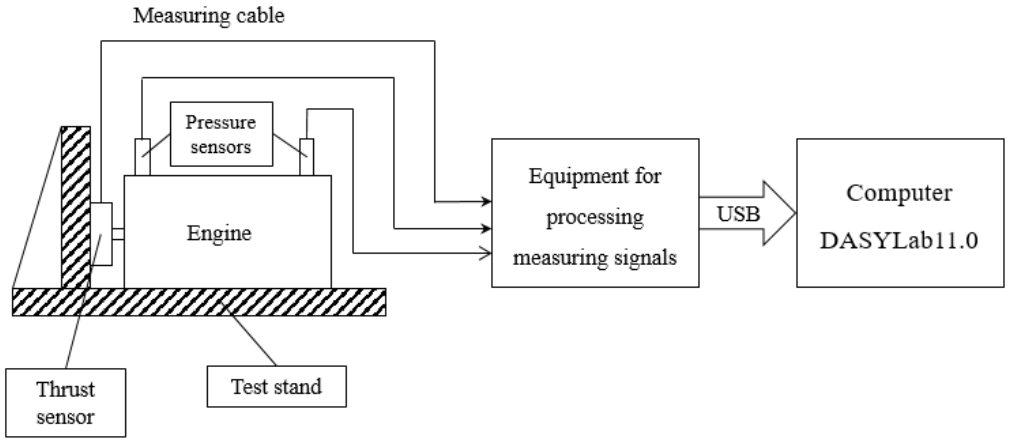

Fig. 7. Scheme of the test stand

Testing the sample engine on the test stand with 2 shots. The laws of thrust and pressure are shown in Fig. 8 and Fig. 9.

Environmental conditions while testing: temperature: 31.2^{o}C, humidity: 70.8%

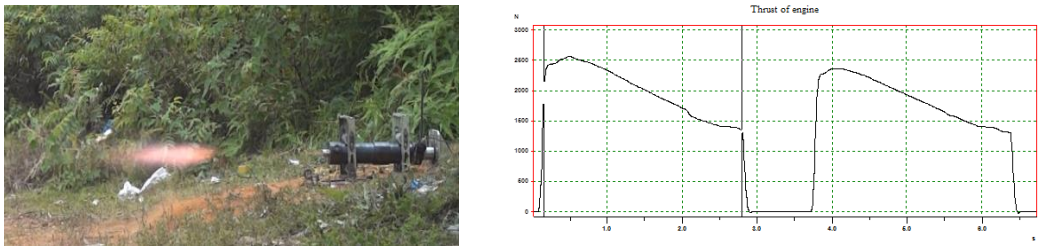

Fig. 8. Sample engine on stand and thrust of engine

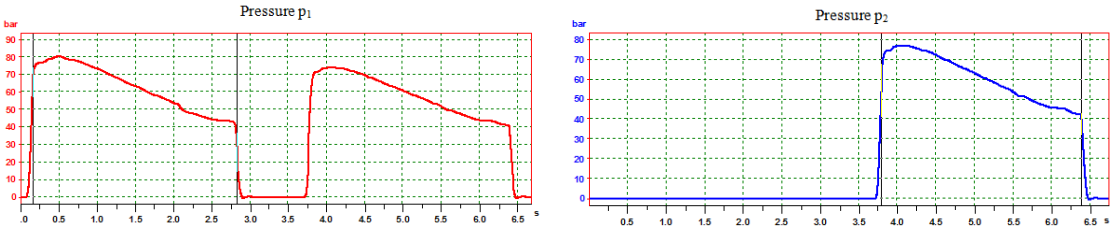

Fig. 9. Pressures in combustion chambers

Test results summary and comparison with theoretical calculation results are presented in Tables 3 and 4.

Table 3. Comparison pressure measurement results and theoretical calculations

	Phase I			Phase II					
Type	p_{11max} (MPa)	p_{11av} (MPa)	t_{11} (s)	p_{12max} (MPa)	p_{12av} (MPa)	t_{12} (s)	p_{22max} (MPa)	p_{22av} (MPa)	t_{22} (s)
Shot 1	8.07	6.38	2.67	7.41	5.93	2.65	7.69	6.18	2.60
Shot 2	8.01	6.41	2.61	7.37	5.79	2.63	7.49	5.88	2.63
Average	8.04	6.40	2.64	7.39	5.86	2.64	7.59	6.03	2.62
Theoretical	7.56	6.75	2.59	6.75	5.62	2.70	6.84	5.67	2.70
Deviation (%)	*6.97*	*5.47*	*1.89*	*8.66*	*4.10*	*2.27*	*9.88*	*5.97*	*3.05*

Table 4. Comparison thrust measurement results and theoretical calculations

	Phase I			Phase II		
Type	P_{max} (N)	P_{av}(N)	$I_{\Sigma 1}$ (Ns)	P_{max} (N)	P_{av}(N)	$I_{\Sigma 2}$ (Ns)
Shot 1	2561	2031	5278	2353	1892	4845
Shot 2	2643	2113	5391	2433	1909	4928
Average	2602	2072	5334,5	2393	1900,5	4886,5
Theoretical	2551	2109	5469	2284	1888	5068
Deviation (%)	*1.96*	*1.79*	*2.52*	*4.55*	*0.66*	*3.71*

After processing the data and taking the average result, comparing with the calculation results, showed that the deviation between the calculation result and the test result was reasonable. Table 3 shows the results of the pressure difference between experimental and theoretical calculations in the range from 1.89% to 9.88%. Table 4 shows the results of the difference of engine thrust between experimental and theoretical calculations in the range from 0.66% to 4.55%. This confirms the reliability of the built mathematical model.

4. Conclusion

The paper has built a mathematical model of internal ballistics calculations for the solid rocket engine with two combustion chambers and performed calculations with the parameters of the model engine.

Theoretical calculation results are verified by experimental studies on sample engines. The experimental results show that the error between experiment and theory is relatively small (less than 10%). This confirms that the built mathematical model has high reliability, as the basis for the next studies for selected engine models.

References

[1] Phạm Thế Phiệt, "*Lý thuyết động cơ tên lửa*," Học viện KTQS, 1995.

[2] Ngô Tuấn Anh, "*Nghiên cứu khai thác phần mềm ASTRA áp dụng cho tính toán các đặc trưng nhiệt động học và xác định một số đặc trưng thuật phóng của động cơ tên lửa nhiên liệu rắn*," Báo cáo tổng kết đề tài KHCN cấp Trung tâm KHKT&CNQS, 2001.

[3] Phạm Thế Phiệt, "Ảnh hưởng của diện tích lỗ thông khí tới lực đẩy trong hệ thống nhiều động cơ tên lửa nhiên liệu rắn," *Tạp chí Khoa học và Kỹ thuật*, số 130, tháng 10/2009.

[4] Oscar Biblarz, George P. Sutton, "Rocket Propulsion Elements," 7th Edition, Wiley-Interscience, *John Wiley & Sons*, 2000.

[5] Шапиро Я.М, Мазинг Г.Ю., Прудников Н.Е. "Теория ракетного двигателя на твердом топливе," *Военное изд*, Москва, 1966.

[6] Абугов Д.И, Бобылев В.М., "Теория и расчет ракетных двигателей твердого топлива," *Машиностроение*, Москва, 1987.

BÀI TOÁN THUẬT PHÓNG TRONG CỦA ĐỘNG CƠ TÊN LỬA NHIÊN LIỆU RẮN HAI BUỒNG ĐỐT

Nguyễn Thế Dũng, Đặng Ngọc Thanh, Nguyễn Ngọc Du

Tóm tắt: *Bài báo trình bày việc xây dựng mô hình lý thuyết bài toán thuật phóng trong cho động cơ tên lửa nhiên liệu rắn hai buồng đốt liên hợp. Từ các đặc trưng làm việc của động cơ tên lửa nhiên liệu rắn hai buồng đốt liên hợp và lý thuyết về động cơ tên lửa nhiên liệu rắn, thiết lập hệ phương trình mô tả các quá trình xảy ra trong các buồng đốt của động cơ. Xây dựng phương pháp giải hệ phương trình và các điều kiện đơn trị cần thiết. Tiến hành giải bài toán trên động cơ mẫu và kiểm chứng kết quả lý thuyết bằng các nghiên cứu thực nghiệm. Sai số giữa các nghiên cứu thực nghiệm và tính toán lý thuyết tương đối nhỏ (nhỏ hơn 10%), khẳng định độ tin cậy của mô hình toán được xây dựng. Kết quả nghiên cứu phục vụ cho việc tính toán thiết kế và chế tạo động cơ tên lửa nhiên liệu rắn hai buồng đốt liên hợp.*

Từ khóa: Động cơ tên lửa nhiên liệu rắn; thuật phóng trong; hai buồng đốt.

Received: 30/9/2020; *Revised:* 13/5/2021*; Accepted for publication:* 17/9/2021

❑